

# Recovery-Free Electron Spin Resonance Observations of NBTI Degradation

J.T. Ryan and P.M. Lenahan  
The Pennsylvania State University  
212 EES Building  
University Park, PA 19490, USA  
phone: 814-863-4630, jtr16@psu.edu

T. Grasser  
Institute for Microelectronics, Technical University of Vienna  
Gusshausstrasse 27-29/E360  
1040 Vienna, Austria

H. Enichlmair  
austriamicrosystems AG  
Schloss Premstaetten, A-8141  
Unterpremstaetten, Austria

**Abstract**— We have developed an approach to perform “on the fly” electron spin resonance (OTF-ESR) measurements of negative bias temperature instability (NBTI) defect generation. This OTF-ESR approach allows for an atomic-scale identification of the defects involved in NBTI free of any recovery contamination. We demonstrate that, during NBTI stressing at elevated temperature and modest negative oxide bias, positively charged oxygen vacancy sites ( $E'$  centers) are generated. Upon removal of the NBTI stressing conditions, the  $E'$  center density quickly recovers to that of its pre-stress values. When similar measurements are made with zero oxide bias at elevated temperature or negative oxide bias at room temperature, the  $E'$  defect density does not change. These observations strongly indicate that NBTI is triggered by inversion layer hole capture at an  $E'$  precursor site which then leads to the depassivation of nearby interface states.

**Keywords:** electron spin resonance, negative bias temperature instability,  $E'$  centers, on the fly

## I. INTRODUCTION AND BACKGROUND

The negative bias temperature instability (NBTI) is perhaps the most important reliability problem facing modern CMOS technology [1-3]. Traditionally, NBTI has been explained in terms of the reaction-diffusion model [1-3]. Although the reaction-diffusion model makes physical sense, many variations of this general idea exist in the literature and none of them are able to fully describe the phenomenon [1-3]. A fundamental and complete understanding of the physical processes involved in NBTI is not yet available.

In the general reaction-diffusion model, a reaction takes place during a negative bias temperature stress (NBTS) which depassivates a silicon-hydrogen bond at the Si/SiO<sub>2</sub> interface [1-3]. A Si/SiO<sub>2</sub> interface state (apparently a P<sub>b</sub> center in pure SiO<sub>2</sub> devices [4, 5]) is created and the hydrogenic species diffuses into the gate stack and into the gate poly silicon; this process leads to the observed shift in threshold voltage and degradation of drive current [1-3]. The observation of NBTI recovery [6-9], a process in which much of the NBTI damage disappears, is explained as the reversal of this process. When the NBTS is removed, some of the hydrogenic species diffuse back to the interface and repassivate the interface states [1-3].

It should be noted that NBTI recovery has only recently been studied in detail [6-9] and is perhaps the most challenging aspect of NBTI. Recent studies of NBTI recovery [6-9] call into question the validity of conclusions drawn in earlier NBTI studies in which recovery was not accounted for. Additionally, recovery cannot be fully explained by the reaction-diffusion model. As noted by Grasser *et al.*, the reaction-diffusion model predicts a universal recovery phenomena nearly independent of the hydrogenic species involved [1]. Additionally, in contrast to some experimental studies [10-13], Grasser *et al.* [1] note that the reaction-diffusion model fails to predict recovery which depends on gate bias, temperature and process conditions.

Recent conventional electron spin resonance (ESR) observations of Fujieda *et al.* [4] on simple Si/SiO<sub>2</sub> capacitors and electrically-detected magnetic resonance (EDMR) observations of Campbell *et al.* [5, 14, 15] on fully processed transistors indicate that in pure SiO<sub>2</sub> structures, NBTI is dominated by Si/SiO<sub>2</sub> interface states (P<sub>b</sub> centers). When subject to very severe NBTS conditions, Campbell *et al.* [5, 14,

---

Work at Penn State supported by Texas Instruments Custom Funding through the Semiconductor Research Corporation. Part of this work has received funding from the European Community's Seventh Framework Programme under Grant Agreement No. 216436 (project ATHENIS).

15] also observed E' center generation. Although their experimental observations are somewhat tenuous, Campbell *et al.* suggest that E' centers could trigger the NBTI process via an E' center/P<sub>b</sub> center hydrogen exchange [5, 14, 15]. This general idea, that NBTI is caused by an E'/P<sub>b</sub> center hydrogen exchange triggered by hole capture at an E' site, has been expressed by Lenahan [16, 17] who provides simple thermodynamics based arguments to this effect. He also noted [16, 17] that the correlation between Si/SiO<sub>2</sub> P<sub>b</sub> centers and E' oxide defects frequently observed in ESR studies of variously stressed Si/SiO<sub>2</sub> device structures may be relevant to NBTI degradation. Conley *et al.* had previously proposed a somewhat similar model to explain how oxide trapped holes trigger interface trap generation in MOS radiation damage [18, 19]. The experimental results of Conley *et al.* [20, 21] clearly demonstrate that multiple E'/P<sub>b</sub> center reactions are thermodynamically and kinetically possible. Fig. 1 provides schematic drawings of the two types of interface states commonly found in (100) Si/SiO<sub>2</sub>, the P<sub>b0</sub> (top) and P<sub>b1</sub> (bottom) centers [22]. Both P<sub>b0</sub> and P<sub>b1</sub> centers are silicon dangling bond defects in which the central silicon atom is back-bonded to three other silicon atoms. Both defects are located precisely at the Si/SiO<sub>2</sub> interface. Fig. 2 illustrates schematic drawings of two E' centers commonly found in pure SiO<sub>2</sub>: a neutral oxygen vacancy (top) and a positively charged oxygen vacancy (bottom) [22]. E' centers are silicon dangling bond defects in which the central silicon atom is back-bonded to three oxygen atoms.

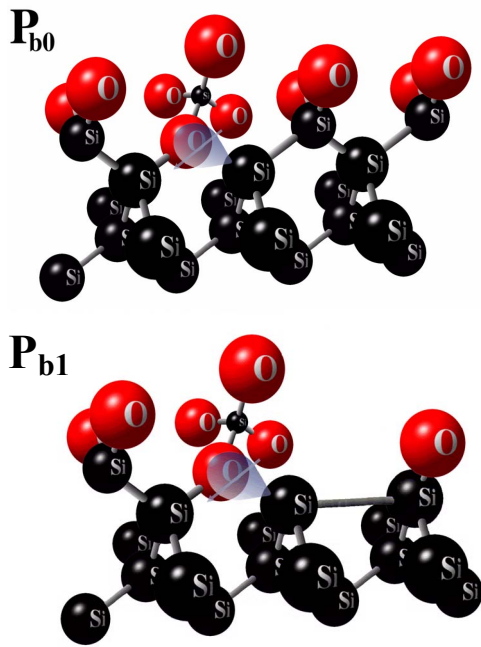


Figure 1. Schematic drawings of P<sub>b0</sub> (top) and P<sub>b1</sub> (bottom) Si/SiO<sub>2</sub> interface states. P<sub>b0</sub> and P<sub>b1</sub> defects dominate interface trapping in (100) Si/SiO<sub>2</sub>. Both are silicon dangling bond defects in which the central silicon atom is back-bonded to three other silicon atoms. The main differences between them are their dangling bond axis of symmetry and electronic density of states [23-27].

Fig. 3a schematically illustrates a Si/SiO<sub>2</sub> interface before (Fig. 3a) and after (Fig. 3b) oxide stressing. The interface of Fig. 3a is typical of oxides which received a forming gas anneal

following thermal oxidation of SiO<sub>2</sub>; Si/SiO<sub>2</sub> P<sub>b</sub> interface states are hydrogen passivated. Lenahan [16, 17] argues that if the oxide stress generates a large number of E' oxide defects (Fig. 3b), and if the bonding energies of the Si-H bond at the hydrogen passivated P<sub>b</sub> center and a Si-H bond at a hydrogen passivated E' center are about the same, the illustration of Fig. 3b is thermodynamically unstable. That is, completely hydrogen passivated P<sub>b</sub> centers in the vicinity of completely unpassivated E' centers is thermodynamically unstable.

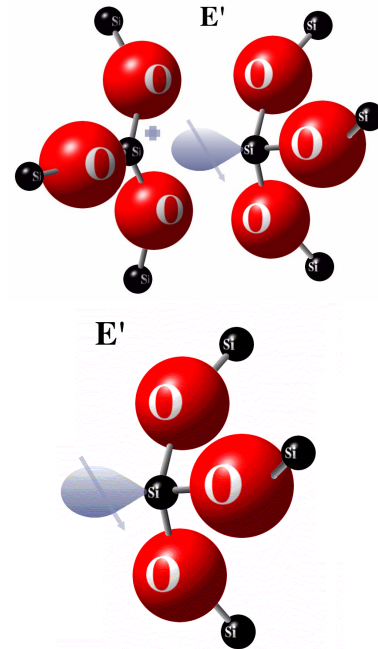


Figure 2. Schematic drawings of two E' centers commonly found in pure SiO<sub>2</sub>: a neutral oxygen vacancy (top) and a positively charged oxygen vacancy (bottom). E' centers dominate charge trapping in pure SiO<sub>2</sub> dielectrics. They are silicon dangling bond defects in which the central silicon atom is back-bonded to oxygen atoms.

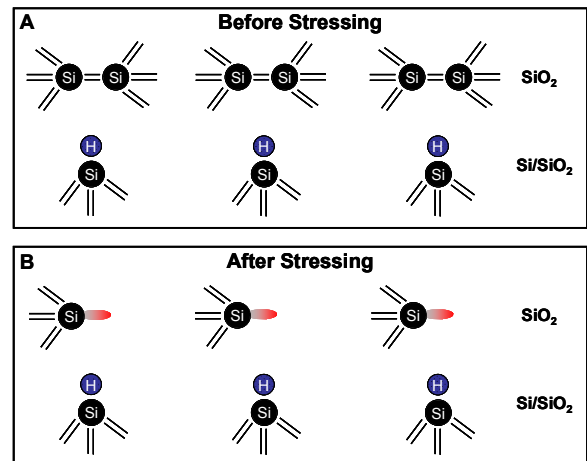


Figure 3. Two simplified illustrations of the Si/SiO<sub>2</sub> interface. (a) A perfect interface prior to stressing in which all P<sub>b</sub> center precursors are hydrogen passivated. (b) After oxide stressing which created large numbers of E' centers in the oxide. Note that the post-stressing illustration (b) is thermodynamically unstable.

The Gibbs free energy of the system:

$$G = H - TS, \quad (1)$$

where  $H$  is enthalpy (sum of energy plus pressure times volume),  $T$  is absolute temperature, and  $S$  is entropy, would be lowered if some hydrogen from the passivated  $P_b$  centers transfers to some of the unpassivated  $E'$  centers in the oxide [16, 17]. This hydrogen transfer would cost little energetically and thus little enthalpy since the two bond energies are roughly equal [16, 17].

However, the hydrogen transfer would greatly increase the entropy of the system; since the entropy of the system is defined as

$$S = k \ln(\Omega), \quad (2)$$

where  $k$  is Boltzmann's constant and  $\Omega$  is the number of microscopic configurations responsible for the macroscopic system, the configurational entropy would increase from  $k \ln(1)$  for the case of Fig. 3b to  $k \ln(M)$ , a large increase, if one hydrogen was removed from any of the  $M$  hydrogen passivated  $P_b$  center sites. [16, 17]. The removal of a second hydrogen would lead to a configurational entropy of  $k \ln[(M)(M-1)/2]$  and so on for additional removal of hydrogen. Additionally, the configurational entropy due to the unpassivated  $E'$  centers would increase from  $k \ln(1)$  to  $k \ln(N)$ , a large increase, if one hydrogen were added to any of the  $N$  unpassivated  $E'$  center sites [16, 17]. This is schematically illustrated in Fig. 4.

Thus, these simple statistical thermodynamics arguments [16, 17] indicate that the transfer of hydrogen from passivated interface states to unpassivated oxide defects is thermodynamically favored and provides a very plausible explanation for the triggering mechanisms of NBTI.

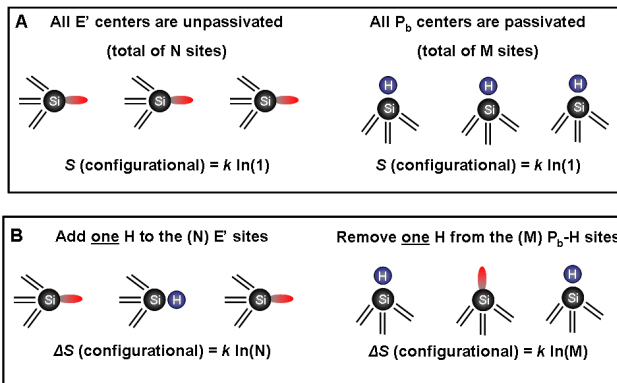


Figure 4. (a) A schematic illustration of an oxide with  $N$  unpassivated  $E'$  center sites and  $M$  hydrogen passivated  $P_b$  center sites. In both cases, the configurational entropy,  $S$ , is given by  $k \ln(1)$ . (b) A schematic illustration of the effect of transferring one hydrogen from a passivated  $P_b$  center site to an unpassivated  $E'$  center site. In both cases, there is a large increase in the configurational entropy.

Quite recently, Grasser *et al.* [28] have developed a comprehensive quantitative two-stage model for NBTI in pure  $\text{SiO}_2$  devices based on these ideas [14-17]. In the Grasser *et al.* model, NBTI is triggered by inversion layer hole capture at an  $E'$  center precursor site (a neutral oxygen vacancy). In the

model proposed by Grasser *et al.*, the NBTI degradation process is initiated (stage one) when inversion layer hole capture occurs at  $E'$  precursor sites (neutral oxygen vacancy) [28]. The hole capture leads to positively charged  $E'$  centers (paramagnetic defects observable with ESR) in the oxide, similar to the schematic drawing provided in Fig. 3b. In stage one, the system is in a recoverable state where the positively charged  $E'$  center can very quickly emit a hole leading to full recovery back to the precursor state.

Grasser *et al.* argue that this recoverable charge trapping state is responsible for NBTI recovery in which much of the damage very quickly heals once the NBTI stress is removed [28]. However, if the NBTI stress is maintained, the system can also proceed to stage two of the model (permanent degradation). Following the arguments [16, 17] discussed above, Grasser *et al.* note that the large number of unpassivated  $E'$  centers in the vicinity of hydrogen passivated  $P_b$  interface states in stage one is thermodynamically unstable. The oxide silicon dangling bonds ( $E'$  centers) created in the stage one process triggers the creation of  $P_b$  centers through the  $P_b/E'$  hydrogen exchange process discussed above [28]. This leads to a poorly recoverable  $P_b$  interface state and the transferred hydrogen essentially "locks in" the positive charge on the  $E'$  center site (rendering it diamagnetic and unobservable with ESR).

The positively charged  $E'$  center and the newly created  $P_b$  interface state in the Grasser *et al.* model is consistent with much of the NBTI literature [1-3] suggesting the degradation is due to interface state generation and/or oxide charge build up. The interface state generation aspect of the model is consistent with the magnetic resonance observations of Campbell *et al.* [5, 14, 15] and Fujieda *et al.* [4] who indicate that NBTI is dominated by interface state generation ( $P_b$  centers). Additionally, the model is consistent with the somewhat tenuous arguments of Campbell *et al.* [5, 14, 15] who observed  $E'$  centers following very harsh NBTI stress and suggest that  $E'$  centers may play an important role in NBTI degradation.

The comprehensive quantitative model of Grasser *et al.* [28] explains NBTI degradation over a wide range of bias voltage and stress temperature, the observed asymmetry between stress and recovery, and the strong sensitivity to bias and temperature during recovery. Perhaps more importantly, the model attributes recovery to charge trapping/detrapping via a non-radiative multi-phonon process [29], which accurately predicts both the very fast and slow recovery phenomena [6-9, 30], due to a very broad distribution of time constants. Since the reaction-diffusion model relies on diffusion of hydrogenic species (a much slower process than tunneling) to account for recovery, it predicts a much slower recovery which is incompatible with experimental observations [6-9]. Additionally, the model predicts that paramagnetic  $E'$  centers will be present during stress and will very quickly recover upon removal of stress [28]. However, prior to this work the existence and role of these  $E'$  centers had not yet been conclusively demonstrated.

As mentioned previously, Campbell *et al.* were only able to report somewhat tenuous  $E'$  experimental observations in NBTI stressed devices [14, 15]. This is so for two reasons.

First, and most importantly, the EDMR technique of spin dependent recombination (SDR) used [31, 32] does not permit observations at significant negative bias; the stress biasing conditions must be altered so that electron and hole quasi Fermi levels are split more or less symmetrically about the intrinsic Fermi level at the Si/SiO<sub>2</sub> interface (that is, the stress biasing must be changed in order to make the measurement and thus introduces recovery). Secondly, SDR is only marginally adequate for E' center detection because only those E' centers very close to the interface can contribute to SDR. Conventional ESR does permit E' center detection at any gate bias if the center is positively charged, as should be the case under stress conditions. In this work, we utilize a newly developed on-the-fly ESR technique to detect positively charged E' centers during NBTI stressing of MOS structures. The newly developed technique permits a recovery free glimpse into the dynamics of NBTI and our results provide insight into the E'/P<sub>b</sub> center NBTI triggering mechanisms discussed above.

## II. EXPERIMENTAL DETAILS

The samples used in this study are simple Si/SiO<sub>2</sub> blanket wafers with 49.5nm thermally grown SiO<sub>2</sub> oxides. The samples received a forming gas anneal following thermal oxidation. ESR measurements were performed before, during, and after the samples were subjected to a NBTS of V<sub>G</sub> = -25V (<5MV/cm oxide electric field) at 100°C. OTF-ESR measurements were performed by first applying negative gate bias via corona ions and then loading the biased samples into a heated quartz dewar situated inside the ESR microwave resonance cavity. The gate bias was monitored before and after stress with a Kelvin probe. ESR measurements were made on a commercially available Bruker Instruments X-band spectrometer with a TE<sub>104</sub> microwave cavity and a calibrated weak pitch spin standard. Some measurements also utilized a calibrated SiO<sub>2</sub> E' standard [33].

## III. RESULTS AND DISCUSSION

Fig. 5 illustrates pre-stress ESR spectra for the forming gas annealed sample (bottom trace) and a nearly identical sample which did not receive a forming gas anneal (top trace) at identical spectrometer gain. The spectrometer settings used were chosen to permit the observation of both P<sub>b</sub> and E' defects and are not optimized for either defect. The sample which did not receive the forming gas (top trace) displays three spectra with g = 2.0063 (P<sub>b0</sub> Si/SiO<sub>2</sub> interface states), g = 2.0036 (P<sub>b1</sub> Si/SiO<sub>2</sub> interface states), and g = 2.0006 (E' oxide defects). The sample which did receive the forming gas anneal (bottom trace) displays a much weaker signal with g = 2.0069 which is consistent with a low density of Si/SiO<sub>2</sub> P<sub>b0</sub> centers. The second integral of the ESR signal is proportional to the number of defects present and, as expected, the forming gas annealed sample has far fewer defects present. Since Si/SiO<sub>2</sub> samples which did not receive forming gas anneals are not technologically relevant, only results taken on the sample which did receive the forming gas anneal are shown in the remainder of this chapter.

Fig. 6 illustrates three ESR traces taken at room temperature for the sample with forming gas. The top trace

was taken on the as-processed sample, the middle trace was taken with the sample biased with -25V at room temperature (bias maintained for several hours during measurement), and the bottom trace taken after removing the negative bias. The room temperature corona bias of -25V (middle trace) does not result in an increase of interface states (P<sub>b</sub> centers) or oxide defects (E' centers). It does, of course, suppress the P<sub>b0</sub> signal because these defects are interface traps and can respond to the substrate silicon Fermi level [23]. (The negative bias renders most of the P<sub>b0</sub> centers positive and diamagnetic and thus ESR inactive.) Fig. 7 illustrates three ESR traces taken at zero volts bias for the sample. The top trace was taken on the as-processed sample at room temperature, the middle trace was taken with the sample at elevated temperature (100°C), and the bottom trace taken after returning the sample to room temperature. The elevated temperature at zero volts bias (middle trace) does not result in an increase of interface states or oxide defects.

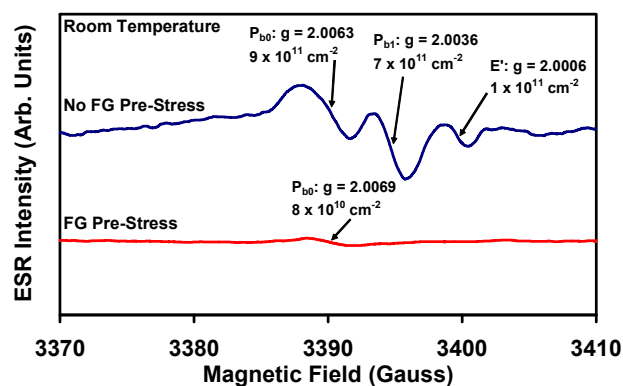


Figure 5. Comparison of pre-stress ESR spectra plotted with identical spectrometer gain for the sample treated with forming gas (bottom trace) and a nearly identical sample which was not treated with forming gas following oxidation (top trace). As expected, the sample which received the forming gas anneal is of much higher quality. (The overlapping P<sub>b0</sub> and P<sub>b1</sub> spectra results in a slightly lower P<sub>b0</sub> g value in the non forming gas annealed sample.)

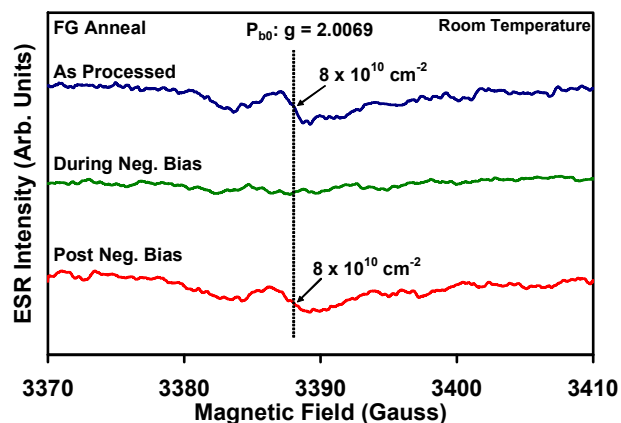


Figure 6. Room temperature ESR traces taken on the sample which received a forming gas anneal as-processed (top trace), with -25V bias (middle trace), and after removal of negative bias (bottom trace). Note that the negative bias alone does not generate additional P<sub>b</sub> interface states or E' defects within the resolution of the measurement.

Fig. 8 illustrates three OTF-ESR traces taken before (top trace), during (middle trace) and after (bottom trace) NBTI stressing ( $V_G = -25V$  and  $T = 100^\circ C$ ) on the FG annealed sample. As mentioned previously, in the as-processed case (top trace) we observe a weak spectrum consistent with Si/SiO<sub>2</sub> P<sub>b0</sub> centers. During NBTI stress (middle trace), we observe the clear generation of Si/SiO<sub>2</sub> P<sub>b1</sub> centers ( $g = 2.0034$ ) and SiO<sub>2</sub> E' centers (2.0006). Upon removal of the stress, the  $g = 2.0006$  E' center signal completely recovers while some of the P<sub>b1</sub> centers remain. This result clearly demonstrates that positively charged E' centers are generated during NBTI stress and very quickly recover upon removal of the stress; that is, positively charged oxygen vacancy sites are generated during stress and very quickly recover. Furthermore, in contrast to Fig. 6 (negative bias only) and Fig.7 (elevated temperature only), the positively charged E' centers are only present when both elevated temperature and negative bias are applied. The fast recovery phenomenon observed also explains the absence of E' center spectra in previous SDR NBTI studies at moderate stress conditions [4, 5, 14, 15]; since SDR is a relatively slow measurement and since the stress biasing conditions must be altered, a large amount of E' center recovery is introduced.

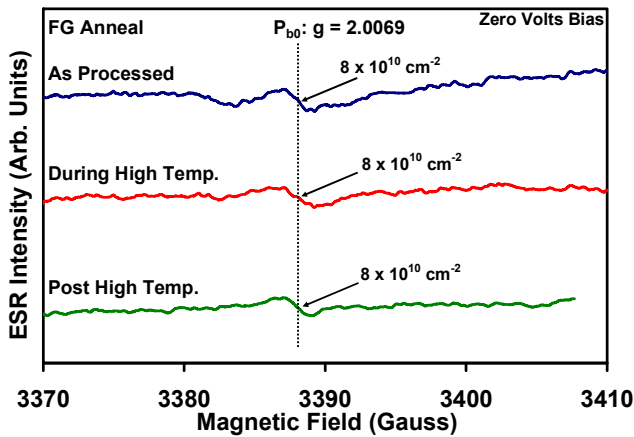


Figure 7. Three ESR traces for the sample which received the forming gas anneal as-processed (top trace), with zero volts bias at 100°C (middle trace), and after cooling the sample back to room temperature (bottom trace). Note that the elevated temperature alone does not generate additional Pb interface states or E' defects.

As mentioned previously, the spectrometer settings used in Figs. 5-8 were chosen to permit the observation of both Si/SiO<sub>2</sub> P<sub>b</sub> centers and SiO<sub>2</sub> E' centers and are not optimized for either defect; the E' center density is underrepresented in these traces. (There is a significant difference in E' and P<sub>b</sub> spin lattice relaxation times which leads to this under-representation [34].) In an attempt to further demonstrate that E' centers (positively charged oxygen vacancy sites) are present during NBTI stressing, Fig. 9 shows three OTF-ESR traces taken on the forming gas annealed sample before (top trace), during (middle trace) and after NBTI stressing (bottom trace). In this figure, the spectrometer settings are optimized for the observation of E' centers. When NBTI stressing is applied (middle trace), a clear signal with  $g_{||} = 2.0016$  and  $g_{\perp} = 2.0006$  appears which is characteristic of an E' center. Upon removal of the NBTI

stress (bottom trace), the E' signal completely recovers. Fig. 10 further demonstrates the identification of this signal as due to an E' center by comparing the during NBTI stress spectra of Fig. 9 (top trace) with that of a commercially available E' standard (bottom trace) [33]. Note the close correspondence between the g values and the line shapes which are characteristic to this type of defect.

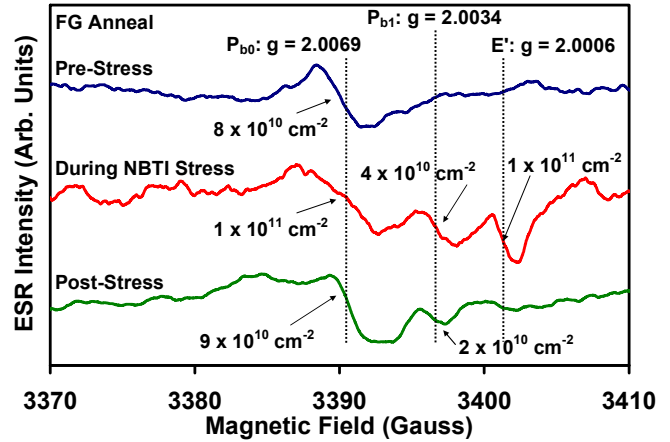


Figure 8. Three ESR traces for the sample which received the forming gas anneal. Note the clear generation of an E' signal during NBTI stress (middle trace), as well as P<sub>b1</sub> center generation, and the nearly complete recovery of the E' defects post-stress (bottom trace).

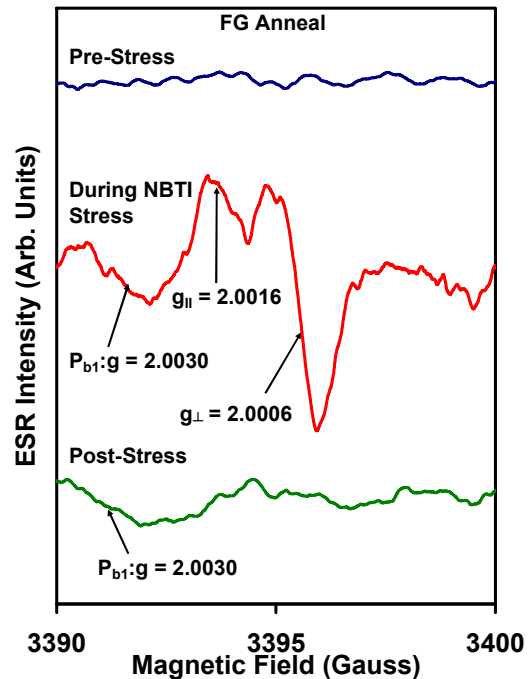


Figure 9. Three ESR traces taken on the sample which received the forming gas anneal. In these traces, the spectrometer settings are optimized to observe E' centers. Note the clear generation of an E' spectrum ( $g_{||} = 2.0016$  and  $g_{\perp} = 2.0006$ ) during stress (middle trace) and its subsequent recovery post-stress (bottom trace).

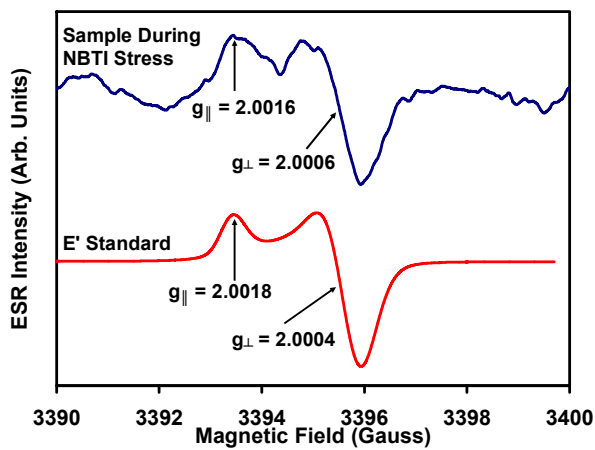


Figure 10. Comparison of the forming gas annealed sample during NBTI stress from Fig. 9 (top trace) and a commercially available E' standard (bottom trace). The standard sample signal-to-noise is much higher because the standard has orders of magnitude more E' centers. Note the close correspondence between the g values and line shapes. The gain of the sample trace is approximately 10,000 times larger than that used for the E' standard; all other spectrometer settings are identical. (Note that the precision of g is  $\pm 0.0002$ .)

#### IV. CONCLUSIONS

In summary, we present results which demonstrate that E' centers are generated in Si/SiO<sub>2</sub> MOS structures when subjected to modest negative oxide bias at elevated temperature. We further demonstrate that these E' centers recover once the stressing conditions are removed. Only the combination of negative oxide bias and elevated temperature results in E' center generation. These results are consistent with and strongly support the suggestions of Campbell et al. [14, 15] and Lenahan [16] as well as the more recent comprehensive two-stage model proposed by Grasser et al. [28] in which NBTI is triggered by the tunneling of electrons from a neutral E' center precursor to unoccupied valence band states. Our results also clearly support (and also provide an explanation for) previously reported results indicating that the very rapid portion of recovery involves the annihilation of oxide trapped holes.

#### REFERENCES

- [1] T. Grasser, W. Goes, and B. Kaczer, "Toward engineering modeling of negative bias temperature instability," in *Defects in Microelectronic Materials and Devices*, D. M. Fleetwood, S. T. Pantelides, and R. D. Schrimpf, Eds. Boca Raton, London, New York: CRC Press, 2009, pp. 399-436.
- [2] G. LaRosa, "Negative bias temperature instabilities in pMOSFET devices," in *Reliability Wearout Mechanisms in Advanced CMOS Technologies*, A. W. Strong, E. Y. Wu, R. P. Vollertsen, J. Sune, G. LaRosa, S. E. Rauch, and R. P. Sullivan, Eds. Hoboken: Wiley, 2009, pp. 331-439.
- [3] D. K. Schroder, "Negative bias temperature instability: What do we understand?," *Microelectronics Reliability*, pp. 841-852, 2007
- [4] S. Fujieda, Y. Miura, M. Saitoh, E. Hasegawa, S. Koyama, and K. Ando, "Interface defects responsible for NBTI in plasma-nitrided SiON/Si(100) systems," *Applied Physics Letters*, pp. 3677-3679, 2003
- [5] J. P. Campbell, P. M. Lenahan, C. J. Cochrane, A. T. Krishnan, and S. Krishnan, "Atomic-scale defects involved in NBTI," *IEEE Transactions on Device and Materials Reliability*, pp. 540-557, 2007

- [6] G. Chen, M. F. Li, C. H. Ang, J. Z. Zheng, and D. L. Kwong, "Dynamic nbtI of p-MOS transistors and its impact on MOSFET scaling," *IEEE Electron Device Letters*, pp. 734-736, 2002
- [7] M. Ershov, S. Saxena, H. Karbasi, S. Winters, S. Minehane, J. Babcock, R. Lindley, P. Clifton, M. Redford, and A. Shibkov, "Dynamic recovery of negative bias temperature instability in p-type metal-oxide-semiconductor field-effect transistors," *Applied Physics Letters*, pp. 1647-1649, 2003
- [8] S. Tsujikawa, T. Mine, K. Watanabe, Y. Shimamoto, R. Tsuchiya, K. Ohnishi, T. Onai, J. Yugami, and S. i. Kimura, "Negative bias temperature instability of pMOSFETs with ultra-thin SiON gate dielectrics," *IEEE Int. Reliab. Phys. Symp.*, pp. 183-188, 2003
- [9] W. Abadeer and W. Ellis, "Behavior of NBTI under ac dynamic circuit conditions," *IEEE Int. Reliab. Phys. Symp.*, pp. 17-22, 2003
- [10] M. Ershov, R. Lindley, S. Saxena, A. Shibkov, S. Minehane, J. Babcock, S. Winters, H. Karbasi, T. Yamashita, P. Clifton, and M. Redford, "Transient effects and characterization methodology of negative bias temperature instability in pMOS transistors," *IEEE Int. Reliab. Phys. Symp.*, pp. 606-607, 2003
- [11] B. Kaczer, V. Arkipov, R. Degraeve, N. Collaert, G. Groeseneken, and M. Goodwin, "Disorder-controlled-kinetics model for negative bias temperature instability and its experimental verification," *IEEE Int. Reliab. Phys. Symp.*, pp. 381-387, 2005
- [12] H. Reisinger, O. Blank, W. Heinrigs, A. Muhlhoff, W. Gustin, and C. Schlunder, "Analysis of NBTI degradation- and recovery-behavior based on ultra fast VT-measurements," *IEEE Int. Reliab. Phys. Symp.*, pp. 448-453, 2006
- [13] C. Shen, M. F. Li, C. E. Foo, T. Yang, D. M. Huang, A. Yap, G. S. Samudra, and Y. C. Yeo, "Characterization and physical origin of fast vth transient in NBTI of pMOSFETs with SiON dielectric," *IEEE IEDM Technical Digest*, pp. 333-336, 2006
- [14] J. P. Campbell, P. M. Lenahan, A. T. Krishnan, and S. Krishnan, "Observations of NBTI-induced atomic-scale defects," *IEEE Transactions on Device and Materials Reliability*, pp. 117-122, 2006
- [15] J. P. Campbell, P. M. Lenahan, A. T. Krishnan, and S. Krishnan, "Direct observation of the structure of defect centers involved in the negative bias temperature instability," *Applied Physics Letters*, pp. 204106, 2005
- [16] P. M. Lenahan, "Atomic scale defects involved in MOS reliability problems," *Microelectronic Engineering*, pp. 173-181, 2003
- [17] P. M. Lenahan, "Deep level defects involved in MOS device instabilities," *Microelectronics Reliability*, pp. 890-898, 2007
- [18] J. F. Conley and P. M. Lenahan, "Molecular-hydrogen, E' center hole traps, and radiation-induced interface traps in MOS devices," *IEEE Transactions on Nuclear Science*, pp. 1335-1340, 1993
- [19] J. F. Conley, P. M. Lenahan, B. D. Wallace, and P. Cole, "Quantitative model of radiation induced charge trapping in SiO<sub>2</sub>," *IEEE Transactions on Nuclear Science*, pp. 1804-1809, 1997
- [20] J. F. Conley, P. M. Lenahan, A. J. Lelis, and T. R. Oldham, "Electron spin resonance evidence that e'(gamma) centers can behave as switching oxide traps," *IEEE Transactions on Nuclear Science*, pp. 1744-1749, 1995
- [21] J. F. Conley, P. M. Lenahan, A. J. Lelis, and T. R. Oldham, "Electron spin resonance evidence for the structure of a switching oxide trap: Long term structural change at silicon dangling bond sites in SiO<sub>2</sub>," *Applied Physics Letters*, pp. 2179-2181, 1995
- [22] P. M. Lenahan and J. F. Conley, "What can electron paramagnetic resonance tell us about the Si/SiO<sub>2</sub> system?," *Journal of Vacuum Science and Technology B*, pp. 2134-2153, 1998
- [23] J. P. Campbell and P. M. Lenahan, "Density of states of P<sub>bi</sub> Si/SiO<sub>2</sub> interface trap centers," *Applied Physics Letters*, pp. 1945-1947, 2002
- [24] J. W. Gabrys, P. M. Lenahan, and W. Weber, "High-resolution spin-dependent recombination study of hot-carrier damage in short-channel mosfets - si<sup>29</sup> hyperfine spectra," *Microelectronic Engineering*, pp. 273-276, 1993
- [25] T. D. Mishima and P. M. Lenahan, "A spin-dependent recombination study of radiation-induced P<sub>bi</sub> centers at the (001) Si/SiO<sub>2</sub> interface," *IEEE Transactions on Nuclear Science*, pp. 2249-2255, 2000

- [26] E. H. Poindexter, G. J. Gerardi, M. E. Rueckel, P. J. Caplan, N. M. Johnson, and D. K. Biegelsen, "Electronic traps and  $P_b$  centers at the Si/SiO<sub>2</sub> interface - band gap energy distribution," *Journal of Applied Physics*, pp. 2844-2849, 1984
- [27] K. L. Brower, "Structural features at the Si/SiO<sub>2</sub> interface," *Z. Phys. Chem.*, pp. 177-189, 1987
- [28] T. Grasser, B. Kaczer, W. Goes, T. Aichinger, P. Hehenberger, and M. Nelhiebel, "A two-stage model for negative bias temperature instability," *IEEE Int. Reliab. Phys. Symp.*, pp. 33-44, 2009
- [29] T. Grasser, H. Reisinger, P. J. Wagner, F. Schanovsky, W. Goes, and B. Kaczer, "The time dependent defect spectroscopy (TDDS) for the characterization of the bias temperature instability," *IEEE Int. Reliab. Phys. Symp.*, pp. 2010
- [30] B. Kaczer, T. Grasser, J. Martin-Martinez, E. Simoen, M. Aoulaiche, P. J. Roussel, and G. Groeseneken, "NBTI from the perspective of defect states with widely distributed time scales," *IEEE Int. Reliab. Phys. Symp.*, pp. 55-60, 2009
- [31] D. Kaplan, I. Solomon, and N. F. Mott, "Explanation of large spin-dependent recombination effect in semiconductors," *Journal De Physique Lettres*, pp. L51-L54, 1978
- [32] D. J. Lepine, "Spin-dependent recombination on silicon surface," *Physical Review B*, pp. 436-441, 1972
- [33] "E' standard available from wilmad lab glass."
- [34] P. M. Lenahan and P. V. Dressendorfer, "Hole traps and trivalent silicon centers in metal-oxide silicon devices," *Journal of Applied Physics*, pp. 3495-3499, 1984